

Onset of surface corrugation in molecular scattering from Ag(111)

M. E. M. Spruit, P. J. van den Hoek, E. W. Kuipers, F. H. Geuzebroek, and A. W. Kleyn
FOM-Institute for Atomic and Molecular Physics, Kruislaan 407, 1098 SJ Amsterdam, The Netherlands

(Received 19 October 1988)

Although close-packed metal surfaces are commonly assumed to be flat for beam energies up to about 1 eV, we find that the close-packed Ag(111) surface is considerably corrugated for O₂ at normal energies below 1 eV. The amount of surface corrugation strongly depends on the kind of incident particle (Ar, CO, O₂).

Molecular-beam scattering from surfaces is well suited to study dynamics of gas-surface interactions.^{1,2} Many phenomena in thermal and superthermal molecular scattering (incident energies $E_i < 2$ eV) scale with the energy $E_n (=E_i \cos^2 \theta_i)$ perpendicular to the surface (normal energy), such as, for example, the width of the angular distribution,³ rotational excitation,^{4,5} vibrational excitation,⁶ and sticking.⁷ θ_i is the angle of incidence with respect to the surface normal. One exception is the sticking of N₂ on W(110),⁸ which scales with E_i . The scaling with E_n suggests that the surface can be assumed to be flat (confirmed by He and H₂ scattering⁹) and that the observed angular broadening is due to thermal motion of surface atoms. Clear deviations have not been seen before for molecular-beam scattering from close-packed surfaces. We will present the first experimental and theoretical results on anomalous broadening of angular distributions of O₂ from Ag(111) due to strong surface corrugation, much stronger than we observe for Ar. This indicates that corrugation of the close-packed Ag(111) surface can be important even at energies just above thermal.

As the surface appears to be flat the most frequently used model, to explain beam scattering, is the rather simple hard-cube model.^{10,11} The importance of rotational excitation has been demonstrated experimentally for NO and N₂ on Ag(111).^{4,5,12-14} Therefore, the hard-cube model has been modified to include a rigid-rotor (hard ellipsoid) instead of a spherical particle.¹⁵ Furthermore, the hard-cube model can be extended with a corrugated surface,¹⁶ although this is never combined with the rigid rotor modification. The hard-cube model, and the 2D (two-dimensional) models based on it, can only explain in-plane scattering. More sophisticated models are based on 3D classical trajectory calculations.^{1,2} Both methods will be used to analyze the data presented in this paper.

The experimental setup is described in detail elsewhere.¹⁷ Only a short description will be given here. A supersonic molecular beam is produced by a 100- μ m heatable dc quartz nozzle. Behind two skimmers the beam is chopped into pulses of about 15 μ s by a rotating disk chopper situated 15 cm in front of the target. The use of a chopper gives the possibility to perform time-of-flight (TOF) measurements with a resolution of 2 μ s. By seeding the beam gas in He, and optionally heating the nozzle, it is possible to raise the translational energy of the beam molecules. The beam is directed with a variable angle of incidence θ_i to a Ag(111) single crystal, mounted on a

two-axis goniometer in the center of a ultrahigh vacuum (UHV) chamber. The Ag(111) crystal is sputtered with 500-eV Ar⁺ ions and annealed at 780 K before the measurements were taken. The quality of the crystal surface is checked with specular He scattering, Auger electron spectroscopy (AES), and low-energy electron diffraction (LEED). All experiments were performed at a surface temperature $T_s = 600$ K. The incident as well as the scattered particles are detected by a differentially pumped quadrupole mass spectrometer (QMS), which has an opening angle of 2°, at a distance of 18 cm from the target crystal. The angle of reflection θ_f can be changed by rotating the detector around the crystal. The construction of the apparatus is such that the lowest available $\theta_f = 60^\circ - \theta_i$.

Experimental results of O₂ scattering from Ag(111) are presented in Fig. 1. A 3D spectrum is built up by a stepwise scanning through θ_f , while measuring a 2D TOF spectrum at each θ_f . To be able to obtain more information from such a 3D spectrum, it can also be plotted in a topographical way. The mean final translational energy of the spectrum is determined by first integrating the angular-TOF spectrum over the scattering angle and then determining the mean translational energy from a fit of the integrated spectrum.^{17,18}

The width of the angular distribution can be up to 40° at thermal energies, when the molecular velocity is comparable with the thermal motion of the surface atoms.¹⁹ As is expected for scattering from hard cubes,^{3,10,11} the angular width decreases drastically when the translational energies become superthermal (above 0.1 eV).¹⁷ At further increase of energy, the width is expected to increase again, due to the onset of structure scattering or corrugation. This has not been observed before for molecular scattering. As is shown in Fig. 1 (upper 3D spectrum), we measure for O₂ at $E_i = 1.56$ eV and $\theta_i = 38^\circ$ on Ag(111) a broadening of the angular distribution which is surprisingly large and asymmetric. The lower 3D spectrum in Fig. 1 illustrates that the angular broadening comes up very fast when increasing the incident translational energy from 0.91 eV to 1.56 eV ($\theta_i = 38^\circ$). Figure 2 shows the angular width as a function of incident energy over the full range from thermal up to about 1.5 eV. To emphasize the dramatic broadening with increasing E_n , the Ar curve is shown for comparison. The sensitivity of the broadening to the normal energy is clearly shown by the topographical plots in Fig. 1. From these spectra we conclude that the

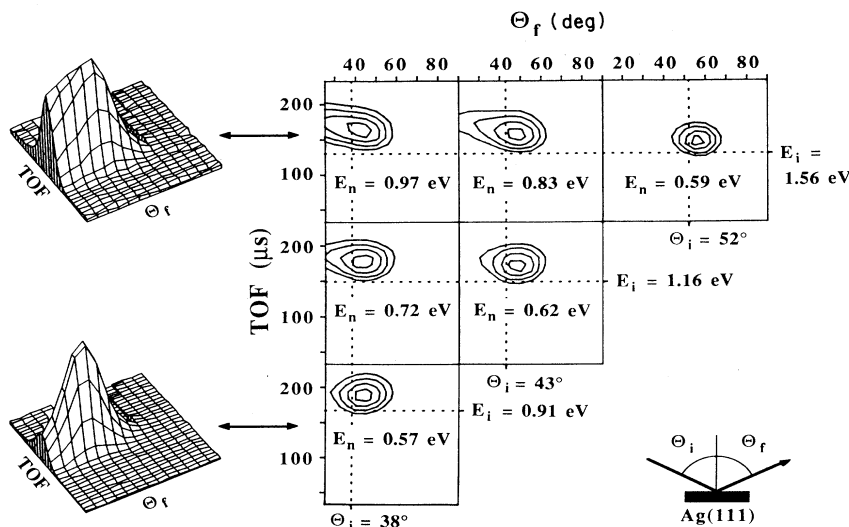


FIG. 1. Topographical representation of intensity of scattered O_2 as a function of θ_f and flight time at different E_i and θ_i . Contour lines are drawn at 30%, 50%, 70%, and 90% of the peak maximum. To the right the angle of incidence decreases, and to the bottom the incident translational energy decreases. The specular positions are indicated by vertical dotted lines and the TOF of the corresponding incident beams are indicated by horizontal dotted lines. For better insight two spectra are plotted as common 3D graphs as well.

angular broadening scales with the normal energy.

Since the strong broadening of the O_2 spectrum at 1.56 eV will be shown to be most likely due to surface corrugation, we can use a modified hard-cube model, which incorporates surface corrugation, to explain the experimental broadening. Such a model, which has been proposed earlier,¹⁶ is based on the common hard-cube model.^{10,11} Using this modified hard-cube model and representing the corrugation by a cosine with an adjustable amplitude, we were able to reproduce the experimental angular distribution for $E_i = 1.56$ eV at $\theta_i = 38^\circ$ ($T_s = 600$ K) when we used a corrugation depth of 0.1 Å at a modulation distance of 2.89 Å, the lattice parameter of Ag. The agreement very sensitively depends on the amount of corruga-

tion, while a variation in the reduced cube mass has only minor effect. We have to emphasize that the corrugation, determined in this way, is an average since we represented the actual 3D corrugation by a 2D corrugation in the model. Consequently, the maximum corrugation amplitude is considerably larger than 0.1 Å; in fact, from our classical trajectory studies follows a maximum corrugation amplitude of 0.45 Å. Since the surface Debye temperature (perpendicular to the surface) is about 120 K,^{20,21} the mean vibrational amplitude of surface atoms is about 0.2 Å at $T_s = 600$ K. Although this value is larger than the mean corrugation that the 1.56 eV O_2 is probing (ca. 0.1 Å), it is smaller than the maximum value. Therefore, thermal roughening of the surface is not the main origin of the angular broadening.

When we measure scattering of other particles (Ar, CO) at approximately $E_i = 1.5$ eV and $\theta_i = 38^\circ$, the width of the angular distribution varies from about 20° for Ar to about 30° for CO, but O_2 exhibits by far the largest broadening ($> 35^\circ$), as is shown in Fig. 2. This indicates that there is a substantial difference in surface corrugation for those particles. Trajectory calculations show that differences in surface corrugation are due to differences in slope of the interaction potential between particle and surface, when it is represented by a sum over Born-Mayer potentials [$V(r) = Ae^{-\rho r}$, where r is the distance from the particle to a surface atom]. If the interaction potential has a long repulsive range ($\rho < 4 \text{ \AA}^{-1}$), the turning point of the approaching molecule will be relatively far away from the surface, where the corrugation of the surface potential is somewhat damped out. In case of steep potentials ($\rho > 4 \text{ \AA}^{-1}$) the corrugation becomes more perceptible at the turning point, so corrugation-induced effects can become larger. The differences in angular distributions disappear at very low energies ($E_n < 0.3$ eV), be-

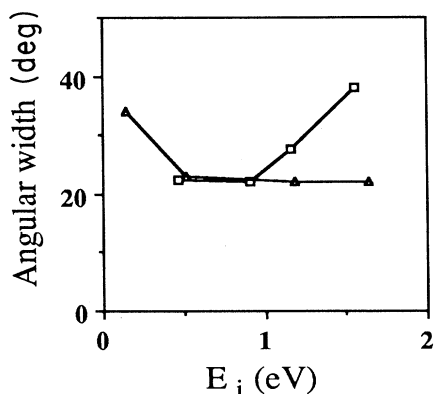


FIG. 2. The full width at half maximum of the angular distribution at $\theta_i = 38^\circ$ as a function of incident energy for O_2 (\square) and Ar (\triangle). The Ar data are in good agreement with earlier experiments (Ref. 3).

cause then the turning point will be far away from the surface.

We have simulated our experimental results by 3D classical trajectory calculations using summed pairwise repulsive interaction potentials.²² These pairpotentials are Born-Mayer potentials fitted to the Hartree-Fock-Slater (HFS) potentials computed for this system.²³ In the O₂/Ag(111) case we used the potential parameters $A=8181$ eV and $\rho=5.03$ Å⁻¹. The value for ρ is unusually large, leading to large corrugation, which is in agreement with our experiments. For Ar the computed $\rho=4.10$ Å⁻¹ which is considerably smaller, leading to less corrugation. The molecular trajectories are calculated at a cluster of 30 Ag atoms, which are incorporated in a thermal Einstein lattice with a temperature of 600 K. Both rotational and vibrational excitation of the initially nonrotating and nonvibrating molecules are included in the calculations. The results of calculations on 1.56 eV incident O₂ on Ag(111) at $\theta_i=38^\circ$ can be seen in Fig. 3. The simulated spectra appear to be in reasonable agreement with the experiments. To show the sensitivity of the trajectory calculations to the kind of potential, we also used the Ziegler-Biersack-Littmark (ZBL) "universal" potential²³ in the calculations. It appeared that there is hardly any agreement between the latter calculations and the experimental results, as can be seen in Fig. 3.

At $\theta_i=38^\circ$ the width of the calculated angular distribution (30°) is lower than the experimentally observed one (38°). Furthermore, the mean translational energy of the scattered molecules ($\langle E_f \rangle_{\text{calc}} \approx 0.9$ eV) is higher than the experimental value ($\langle E_f \rangle_{\text{expt}} \approx 0.7$ eV). These deviations might be due to errors in the potential, either due to an incorrect pair potential, or to a breakdown of the assumed pairwise additivity.²³ Figure 3 clearly shows that the computed results strongly depend on the shape of the pair potential. However, for both Ar and CO scattering at similar energies and for Na scattering in the energy range from 10–100 eV, all from the same surface, the classical trajectory calculations using similar HFS-linear-combination-of-atomic-orbital (LCAO) potentials as computed for Ag-O describe the experimental results very well.^{24,25} This might point to additional energy transfer due to formation of an ionic intermediate (O₂⁻) during the collision, which is not possible in the other cases mentioned and not included in the calculations.²⁶ Formation of O₂⁻ scattering has been observed at much higher incident energies (around 100 eV).²⁷ In gas-phase collisions between K and O₂ an ionic intermediate has been shown to be extremely effective to energy transfer between translation and O₂ vibration.²⁸ This is due to the occurrence of so-called snarled trajectories along the potential energy surface that effectively couple the translational and vibrational degree of freedom. This may lead to the additional energy transfer observed, when comparing data

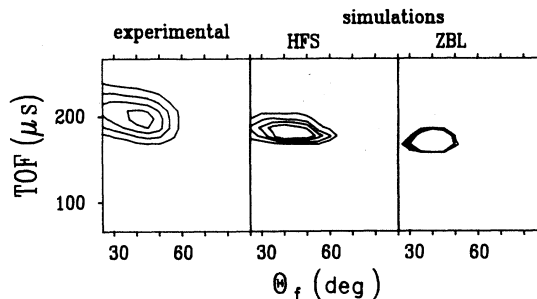


FIG. 3. Calculated angular-TOF spectra of O₂ ($\theta_i=38^\circ$), determined by classical trajectory calculations, compared to the experimental spectrum. The "experimental" parameters are the same as those of the experimental spectrum in Fig. 1 (upper-left spectrum). For comparison the result of classical trajectory calculations, based on the ZBL potential, is shown also.

and results of the trajectory calculations. In these models the lateral degree of freedom is not included. It is not unlikely that when strong coupling between translation and vibration occurs the lateral degree of freedom will also be coupled to translation, leading to an enhanced corrugation compared to a situation where charge transfer and snarled trajectories are ignored.

We conclude that the broadening of the angular distribution can be explained by surface corrugation. The amount of surface corrugation is to a large extent determined by the normal-incident energy and the slope of the molecule-surface interaction potential. For C and O the computed $\rho \approx 5.1$ Å⁻¹, which is surprisingly large for such a system ($\rho_{\text{Ar}}=4.1$ Å⁻¹). The large energy transfer found in the present O₂ experiments and the width of the angular distribution at the largest E_n exceed the computed one and may indicate that negative ion resonances are important for the energy transfer in gas-surface collisions.

After completion and submission of this manuscript similar observations for the interaction between Ar, N₂, and W(100) have been reported.²⁹ The strong difference between O₂ and Ar seen in our work is not seen for Ar and N₂ on W(100).

The authors thank E. J. Baerends for putting the HFS program at their disposal and F. W. Saris for valuable suggestions and comments on the manuscript. This work is part of the research program of the Foundation for Fundamental Research of Matter (Stichting voor Fundamenteel Onderzoek der Materie, FOM) and was made possible by financial support from the Dutch Organization for Advancement of Research (Nederlandse Organisatie voor Wetenschappelijk Onderzoek, NWO).

¹J. A. Barker and D. J. Auerbach, Surf. Sci. Rep. 4, 1 (1985).

²R. B. Gerber, Chem. Rev. 87, 29 (1987).

³D. R. Miller and R. B. Subbarao, J. Chem. Phys. 52, 425 (1970); J. N. Smith, Jr., Surf. Sci. 34, 613 (1973); S. M. Liu, W. E. Rodgers, and E. L. Knuth, in *Rarefied Gas Dynamics*,

edited by M. Becker and M. Fiebig (Deutsche Forschungs- und Versuchsanstalt für Luft- und Raumfahrt e.V., Porz-Wahn, Germany, 1974); H. P. Steinrück and R. J. Madix, Surf. Sci. 185, 36 (1987).

⁴A. W. Kleyn, A. C. Luntz, and D. J. Auerbach, Phys. Rev.

- Lett. **47**, 1169 (1981).
- ⁵G. O. Sitz, A. C. Kummel, and R. N. Zare, *J. Vac. Sci. Technol. A* **5**, 513 (1987); *J. Chem. Phys.* **87**, 3247 (1987).
- ⁶C. T. Rettner, F. Fabre, J. Kimman, and D. J. Auerbach, *Phys. Rev. Lett.* **55**, 1904 (1985).
- ⁷C. T. Rettner, L. A. Delouise, and D. J. Auerbach, *J. Chem. Phys.* **85**, 1131 (1986).
- ⁸H. E. Pfnür, C. T. Rettner, J. Lee, R. J. Madix, and D. J. Auerbach, *J. Chem. Phys.* **85**, 7452 (1986).
- ⁹J. M. Horne and D. R. Miller, *Surf. Sci.* **66**, 365 (1977).
- ¹⁰F. O. Goodman and H. Y. Wachman, *Dynamics of Gas-Surface Scattering* (Academic, New York, 1976).
- ¹¹E. K. Grimmelmann, J. C. Tully, and M. J. Cardillo, *J. Chem. Phys.* **72**, 1039 (1980).
- ¹²F. Frenkel, J. Häger, W. Kruger, H. Walther, C. T. Campbell, G. Ertl, H. Kuipers, and J. Segner, *Phys. Rev. Lett.* **46**, 152 (1981).
- ¹³G. M. McClelland, G. D. Kubiak, H. G. Rennagel, and R. N. Zare, *Phys. Rev. Lett.* **46**, 831 (1981).
- ¹⁴J. Kimman, C. T. Rettner, D. J. Auerbach, J. A. Barker, and J. C. Tully, *Phys. Rev. Lett.* **57**, 2053 (1986).
- ¹⁵J. D. Doll, *J. Chem. Phys.* **59**, 1038 (1973); W. L. Nichols and J. H. Weare, *ibid.* **66**, 1075 (1977); Z. Bacic and S. D. Bosanac, *Chem. Phys. Lett.* **105**, 518 (1984).
- ¹⁶C. Steinbrüchel, *Chem. Phys. Lett.* **76**, 58 (1980); *Surf. Sci.* **115**, 247 (1982).
- ¹⁷M. E. M. Spruit, E. W. Kuipers, M. G. Tenner, J. Kimman, and A. W. Kleyn, *J. Vac. Sci. Technol. A* **5**, 496 (1987).
- ¹⁸K. C. Janda, J. E. Hurst, C. A. Becker, J. P. Cowin, D. J. Auerbach, and L. Wharton, *J. Chem. Phys.* **72**, 2403 (1980).
- ¹⁹H. Asada, *Jpn. J. Appl. Phys.* **19**, 2055 (1980); **20**, 527 (1981).
- ²⁰P. Masri and L. Dobrzynski, *Surf. Sci.* **32**, 623 (1972).
- ²¹C. Kittel, *Introduction to Solid State Physics* (Wiley, New York, 1976).
- ²²P. J. van den Hoek, T. C. M. Horn, and A. W. Kleyn, *Surf. Sci. Lett.* **198**, L335 (1988).
- ²³E. J. Baerends, D. E. Ellis, and P. Ros, *Chem. Phys.* **2**, 41 (1973); P. J. van den Hoek, A. D. Tenner, A. W. Kleyn, and E. J. Baerends, *Phys. Rev. B* **34**, 5030 (1986).
- ²⁴M. E. M. Spruit, P. J. van den Hoek, E. W. Kuipers, F. H. Geuzebroek, and A. W. Kleyn, *Surf. Sci.* (to be published).
- ²⁵T. C. M. Horn, Pan Haochang, P. J. van den Hoek, and A. W. Kleyn, *Surf. Sci.* **201**, 573 (1988).
- ²⁶J. W. Gadzuk, *Comm. At. Mol. Phys.* **16**, 219 (1985); S. Holloway and J. W. Gadzuk, *J. Chem. Phys.* **82**, 5203 (1985); J. W. Gadzuk and S. Holloway, *Phys. Rev. B* **33**, 4298 (1986); D. M. News, *Surf. Sci.* **171**, 600 (1986); S. Holloway, *J. Vac. Sci. Technol. A* **5**, 476 (1987); J. W. Gadzuk, *J. Chem. Phys.* **86**, 5196 (1987).
- ²⁷Pan Haochang, T. C. M. Horn, and A. W. Kleyn, *Phys. Rev. Lett.* **57**, 3035 (1986).
- ²⁸A. W. Kleyn, E. A. Gislason, and J. Los, *Chem. Phys.* **52**, 81 (1980).
- ²⁹C. T. Rettner and E. K. Schweizer, *Surf. Sci. Lett.* **203**, L677 (1988).